ELSEVIER

Journal of Chromatography A, 688 (1994) 135–152

JOURNAL OF CHROMATOGRAPHY A

# Pulsed discharge helium ionization detector Universal detector for inorganic and organic compounds at the low picogram level

W.E. Wentworth[a,*], Huamin Cai[a], Stanley Stearns[b]

[a]*Chemistry Department, University of Houston, 4800 Calhoun Road, Houston, TX 77204-5641, USA*

[b]*Valco Instruments Co., Inc., Houston, TX 77055, USA*

First received 22 June 1994; revised manuscript received 13 September 1994

**Abstract**

The pulsed discharge helium ionization detector is a universal ionization detector with sensitivity in the low picogram range. The response is approximately constant for saturated hydrocarbons on a per gram basis. Unsaturated and aromatic hydrocarbons have lower sensitivities, by about 10–20%. Heterocyclic substituents such as oxygen, chlorine and bromine tend to lower the response on a per gram basis. The dependence of the response on various parameters such as pulse interval and power, voltage, flow-rate and detector volume has been investigated. The response is linearly related to concentration over five orders of magnitude. The detector volume can be made small enough for high-speed microbore chromatography.

## 1. Introduction

In a previous publication the pulsed discharge helium ionization detector (PDHID) was introduced, and its capabilities in the analysis of permanent gases were demonstrated [1]. In other applications —air pollution analysis, for example— the simultaneous analysis of inorganic and organic compounds is desired; nitric oxide and sulfur dioxide need to be detected as well as formaldehyde, aromatic hydrocarbons and halogenated compounds. It is also important to analyze for trace water in organic streams, because water may be deleterious to the catalyst or process. In this paper we demonstrate the response of the PDHID to both inorganic and organic compounds.

Since the PDHID is sensitive and essentially non-destructive (ca. 0.01–0.1% ionization) it can be used in conjunction with more selective detectors of comparable sensitivity. For example, the pulsed discharge source can be adapted to the electron-capture mode, yielding sensitivities on the femtogram level [2]. Also various emission detectors such as microwave-induced plasma [3], alternating current helium plasma, [4] capacitively-coupled plasma [5], radio frequency plasma [6] and helium discharge [7,8], could be used in conjunction with the universal PDHID to detect various elemental compositions and functional groups. (For a general discussion of element-specific chromatographic detection by atomic emission, consult the text

* Corresponding author.

0021-9673/94/$07.00 
*SSDI* 0021-9673(94)00913-9

which compiles the presentations given at a recent ACS symposium [9]).

To evaluate the performance of the PDHID in organic analysis, an appropriate basis for comparison is the flame ionization detector (FID). For inorganic analysis we compare it to the photoionization detector. In a subsequent publication we will demonstrate its use in high-speed chromatography with 0.05–0.10 mm I.D. microbore columns, comparing the results to those obtained with the micro-thermal conductivity detector.

## 2. Experimental

In the previous publication describing the analysis of permanent gases [1], we used a PDHID in which the sample passed through the reaction zone and then through the discharge region. This was satisfactory for the analysis of permanent gases, since decomposition of the inorganic compounds does not contaminate the electrodes. However, this configuration is unsuitable for organic analysis, since extensive analysis leads to contamination of the discharge electrodes. When trace analysis is being carried out with capillary columns, any contamination of the discharge electrodes is negligible.

A schematic diagram of the PDHID used in this study is shown in Fig. 1. The detector is divided into two sections: the discharge section (1.6 mm I.D.) and the reaction section (3 mm I.D.). The reaction section has two ring-shaped electrodes; a negative potential is applied to one, repelling electrons to the other for collection. Because we are demonstrating the use of the PDHID as a universal detector, we use a flow configuration in which only the helium makeup gas passes through the discharge region, minimizing the chance of discharge electrode contamination through contact with organic compounds. (However, if high concentrations of organic compounds are passed through the detector for extended periods of time, some organic material could still diffuse into the discharge region and contaminate the discharge electrodes. Under normal use with capillary columns, contamination of the electrodes is negligible even over extended periods of time). As makeup flow passes through the discharge region into the reaction zone, the analytes exit the GC capillary column directly into the reaction zone near the repelling electrode, flowing counter to the flow of the helium makeup. This configuration lends itself to miniaturization, making it more suitable for capillary column GC.

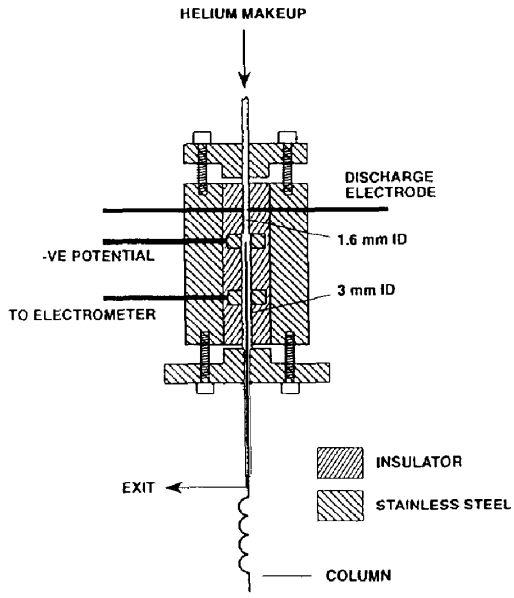


Fig. 1. Schematic diagram of the PDHID used in this study. -VE indicates bias potential.

The analyte is ionized by high-energy photons as it moves through the 10-mm insulating section between the electrodes. The volume of this reaction zone is 113 $\mu$l; that is, the volume of a cylinder with a diameter of 3 mm and a length of 16 mm (3 mm for each electrode + 10 mm for the insulated spacer). A small portion of this volume is occupied by the capillary column. Since the column has an outside diameter ranging from 0.4 mm for microbore columns to 0.8 mm for megabore columns, the volume of the column in the reaction zone ranges from 1.75 to 7.0 $\mu$l, yielding an effective detector volume of approximately 106–111 $\mu$l. In this study we use an AT-5 (formerly RSL-200) bonded phase silica column, 30 m $\times$ 0.25 mm I.D., 1.0 $\mu$m film thickness (Alltech, Deerfield, IL, USA), installed in the

oven of a Varian (Walnut Creek, CA, USA) 1400 gas chromatograph.

Grade 5 (99.999%) helium gas (Trigas, Houston, TX, USA) is used as the capillary column carrier gas as well as the makeup gas that passes through the discharge region. The helium passes through a Valco (Houston, TX, USA) helium purifier, which uses a non-evaporable gettering alloy to remove all impurities except inert gases and nitrogen. (Although water is removed by the helium purifier, emission spectra generally show low levels of OH emission, probably arising from water which enters the helium from the stainless steel tubing connecting the purifier to the detector). The effects of various parameters such as makeup flow-rate, collecting potential and discharge frequency were evaluated using a Scotty II gas mixture of 100 ppm (v/v) of $C_1$–$C_6$ *n*-hydrocarbons in helium (Scott Specialty Gases, Houston, TX, USA).

The coil is charged with 20 V from a Heathkit 2718 tri-power supply unit (Heath, Benton Harbor, MI, USA). The duration of the charge and the pulse frequency are controlled by a 4001 ultravariable pulse generator (Global Specialties, New Haven, CT, USA). The negative potential that repels the electrons to the collecting electrode is supplied by a Keithley (Cleveland, OH, USA) Model 240A high-voltage power supply or a Kepco (Flushing, NY, USA) ABC d.c. supply.

The collection of electrons at the collecting electrode comprises the detector response. This signal is sent to the electrometer of the Varian 1400 GC system, but because the typical standing current for the PDHID (on the order of 1–5 nA) is much larger than the background current expected from an FID, the bucking current in the electrometer is increased to a maximum of 90 nA by changing a resistance from $10^{10}$ to $10^8$ Ω.

The output of the electrometer is connected to a single-channel Houston Instrument (Austin, TX, USA) Omniscribe strip chart recorder Series B-5000 and to a Hewlett-Packard (Avondale, PA, USA) integrator 3390A. The total electrical quantity ($Q$) arising from the ionization of a given analyte can be calculated by integrating the GC peaks; thus, if we know the amount (mol) of analyte injected and assume that one molecule produces one electron after ionization, the ionization efficiency can be determined by the following equation

$$\% \text{ ionization efficiency} = \frac{\text{current (C/s)} \cdot \text{time (s)}/F\ (96\,500\ \text{C/mol})}{\text{mol of analyte in detector (mol)}} \cdot 100\%$$

The product of current × time is the area under the GC peak, which was measured using a Hewlett-Packard integrator 3390A.

Injections are made by a Valco four-port sampling valve with an internal volume of 0.06 μl (determined by an engraving on the rotor), or by a Valco six-port sampling valve with external loops sized from 5–50 μl. A variety of gases and liquids (ca. 99% purity) were used to examine the relative response factors, with the liquids diluted in a solution of a high-boiling solvent such as *n*-decane (Sigma, St. Louis, MO, USA) before injection. The major peak is obvious from the chromatograms.

Measurements of the vacuum UV emission from the discharge source were carried out using a vacuum monochromator (Acton VM502) containing a holographic grating with 1200 grooves/mm. In order to obtain spectra below 120 nm, the pulsed discharge source was mounted directly to the monochromator body, without a window or entrance slit. The discharge is sufficiently narrow that it can serve as the optical image when placed vertically at the focal point of the monochromator. In order to have transparency down to ca. 60 nm, the monochromator was purged with pure helium. Below 60 nm the helium begins to absorb.

## 3. Results and discussion

The PDHID has several variable operating parameters that affect its sensitivity and the linearity of response with concentration. Two of these parameters are associated with the pulsed discharge: (1) the power transmitted to the primary coil of the pulsed high-voltage transformer, which in turn affects the voltage and

current of the discharge; and (2) the frequency or interval of the pulsed discharge. In most of our work we use a 20 V power supply. However, the power to the coil is a product of the duration as well as the voltage of the charge transmitted. The duration is varied by changing the width of the square wave pulse generated by the pulser. Charging times generally range from 15–100 $\mu$s, depending upon the pulse interval, which ranges from 200–1000 $\mu$s. The effects of the two pulse discharge parameters will be discussed shortly.

The other operating parameters that affect the PDHID are: (1) the potential applied to repel the electrons to the collecting electrode; and (2) the helium flow-rate through the discharge region. The effects of these parameters will also be discussed shortly.

### 3.1. Pulsed discharge: interval and power

In this study the electrode separation at the discharge is constant at ca. 1.6 mm; the diameter of the hole through which the helium flows is 1.6 mm (Fig. 1), and the electrodes are adjusted so that their tips are at the walls of this hole. The effect of the power applied to the discharge depends upon the electrode separation.

As explained previously, the power supplied to the discharge via the primary coil is changed by varying the charging time from a 20 V power supply. Fig. 2a shows the detector response to 0.89 ng of propane as a function of the charging time in $\mu$s. (The pulse interval was held constant at 300 $\mu$s). The response, expressed as the percent ionization, increases as the charging time is increased. However, it passes through a maximum of ca. 0.09% ionization at 45 $\mu$s and then decreases.

We also measured the standing current, which arises from the ionization of helium and impurities in the carrier gas, including column bleed. Fig. 2b shows the direct relationship between the percent ionization of propane and the standing current, which varies with the coil charging time. This suggests that the discharge power generates proportional amounts of ionization of the carrier gas (standing current) and of the analyte (detector response).

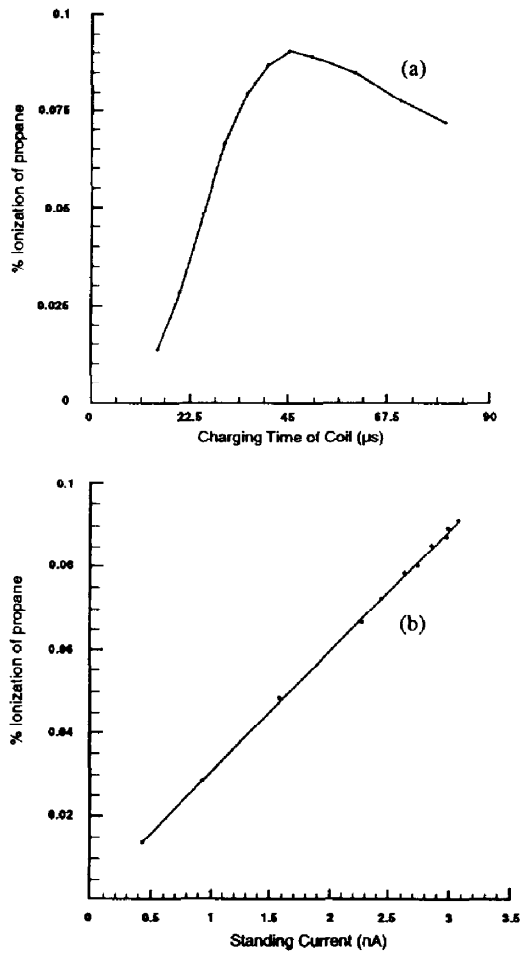


Fig. 2. Detector response in terms of percent ionization versus (a) coil charging time and (b) standing current (which changes with coil charging time); 5.0 $\mu$l of 100 ppm propane (0.89 ng); discharge flow-rate: 20 ml/min; pulse interval 300 $\mu$s.

The percent ionization of propane was also measured as a function of pulse interval, with the charging time constant at 40 $\mu$s. The results are shown in Fig. 3a. Note that the percent ionization remains somewhat constant from 200–50 $\mu$s but then decreases as the pulse period increases, as expected. However, the detector response goes through a second maximum of ca. 0.05% at ca. 500–600 $\mu$s. This behavior is probably related to the *LC* (inductance–capacitance) characteristics of the coil. The standing current was recorded as well; Fig. 3b shows a direct

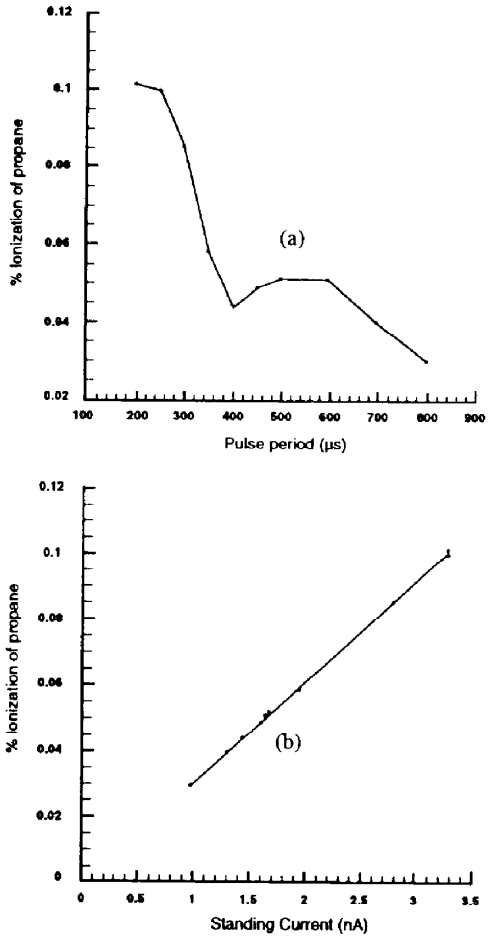


Fig. 3. Detector response in terms of percent ionization versus (a) pulsed discharge interval and (b) standing current (which changes with pulsed discharge interval); 0.89 ng propane, discharge flow-rate: 20 ml/min; charging time of the coil: 40 μs; d.c. voltage to the coil: 20 V.

relationship between the detector response as percent ionization and the standing current, which varies with the pulse interval.

Because detector response and standing current vary proportionally with the input pulse width and period, the effect of these parameters on detector response can be more readily ascertained by simply observing the standing current. More detailed observations of the dependence of the standing current on both the pulse width and period are shown in Fig. 4. Note that when pulse periods in the range of 200–1000 μs are used, the standing current goes through three maxima,

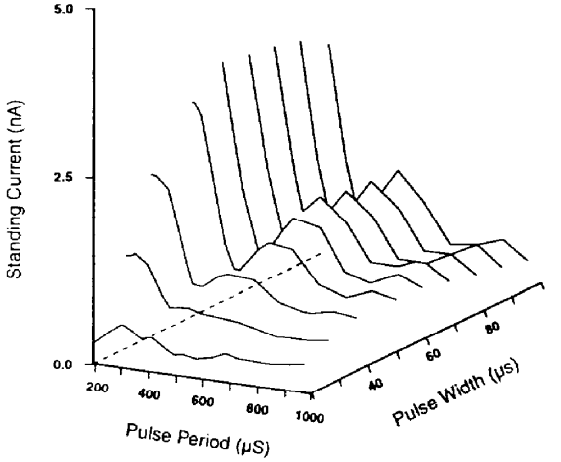


Fig. 4. Effects of pulse width and period on standing current.

regardless of pulse width. These maxima are around 225, 450 and 900 μs, values which correspond to integer multiples of the *LC* resonant frequencies of the discharge circuit. As the pulse period is increased, the three standing current maxima decrease rapidly. A similar relationship between standing current and input pulse width as in Fig. 2a under different pulse periods can also be observed in Fig. 4.

It appears from the data in Fig. 4 that if a higher energy pulse is desired, a charging time of 100 μs or more with a pulse interval of 500 μs is ideal. For the emission mode [12] it may be desirable to have a more energetic discharge at a wider pulse interval of, for instance, 500 μs. For the ionization mode a pulse interval of 200–300 μs with a charging time of 40–50 μs should be most satisfactory since the standing current and response are greater at these conditions. Since the discharge has a short duration (ca. 1 μs) and the pulse period is large (ca. 200–500 μs), the metal electrodes are exposed to the high current for only a small fraction of the time. Consequently, there is no apparent heating in the discharge region.

### 3.2. Bias voltage for electron collection

A constant negative bias voltage is applied to the electrode adjacent to the discharge, as shown in Fig. 1. Fig. 5 is a graph of the response to 0.89

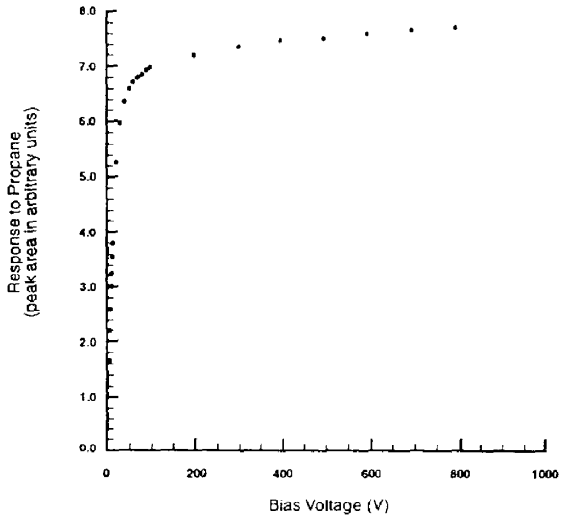


Fig. 5. Detector response (percent ionization) versus bias voltage; 0.89 ng propane; discharge flow-rate: 20 ml/min; pulse interval: 300 $\mu$s; charging time of the coil: 40 $\mu$s; d.c. voltage to the coil: 20 V.

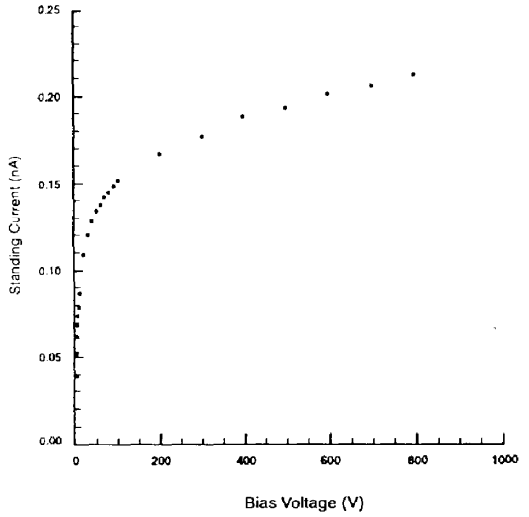


Fig. 6. Standing current versus bias voltage. Discharge flow-rate: 20 ml/min; pulse interval: 300 $\mu$s; charging time of the coil: 40 $\mu$s; d.c. voltage to the coil: 20 V.

ng of propane versus bias or repelling voltage. It appears that the response increases rapidly with increasing voltage, leveling off to a plateau. The region in which the response increases linearly with bias voltage is usually called the *collecting* region, and the region in which the response is independent of bias voltage is usually called the *saturation* region. The PDHID works in the saturation region, in which the noise level is lower. A similar curve is obtained for standing current versus bias voltage, shown in Fig. 6.

### *3.3. Helium flow-rate through the discharge region*

The helium that passes through the discharge region has two purposes: (1) it keeps the discharge region clean so that helium excited species can be generated; and (2) it serves as makeup gas to reduce the residence time of the eluting analyte in the detector. The necessary residence time in the detector is a function of the chromatographic peak width. In order to maintain the integrity of the chromatography, the residence time in the detector should be as short as 10–20% of the peak width. Thus, if the peak width is 5 s the residence time should be 0.5–1 s, which requires a flow-rate of 6.8–13.6 ml/min through a cell with a volume of 113 $\mu$l. If the peaks are as sharp as 1 s width, then the helium flow-rate must be increased to 34–68 ml/min.

Generally as the flow-rate increases the eluting analyte becomes more dilute and the response decreases. If this were the only effect of the helium flow-rate, we would expect the response to vary linearly with the reciprocal flow-rate. Such a graph of the response to propane is shown in Fig. 7, and indeed, there is a linear dependence at high flow-rates. However, at lower flow-rates the curve breaks over and even appears to approach a plateau.

The decrease in response at higher analyte concentrations (lower flow-rates) could be due to saturation of the detector. To eliminate this possibility, response versus helium flow-rate was measured at two different analyte concentrations. This was accomplished using the six-port sampling valve and two sample loops (6 and 50 $\mu$l) to inject the 100 ppm propane mixture. The same shaped curves are obtained (Fig. 7), suggesting that the curvature is not related to concentration.

Further investigation indicated that the plateau in the response vs. 1/flow-rate curve is

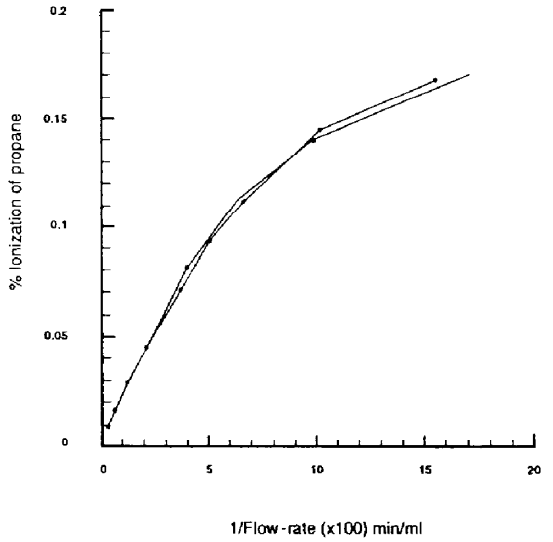


Fig. 7. Detector response (percent ionization) versus reciprocal flow-rate. Pulse interval: 300 $\mu$s; charging time of the coil: 40 $\mu$s; d.c. voltage to the coil: 20 V; bias voltage: 200 V; sample: 100 ppm propane; sample size: (●) 6 $\mu$l, (■) 50 $\mu$l; volume of detector: 113 $\mu$l.

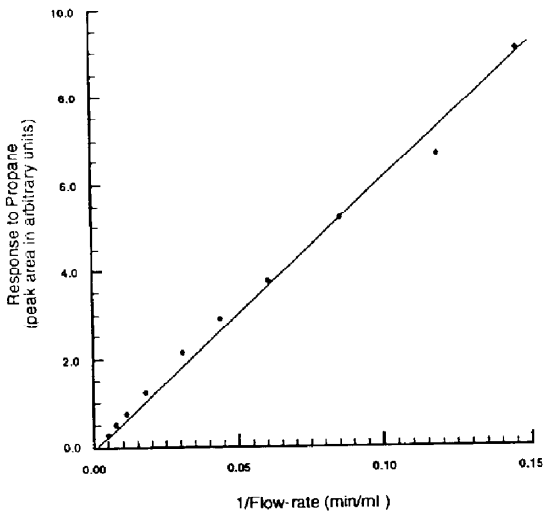


Fig. 8. Detector response (peak area in arbitrary units) versus reciprocal flow-rate under constant detector pressure (6 p.s.i.; 1 p.s.i. = 6894.76 Pa).

due to changes in detector pressure and in the amount of air back-diffusion as the flow-rate changes: the lower the flow-rate, the higher the air back-diffusion and the lower the detector pressure. Since both these factors contribute to decreased detector response, they offer a likely explanation for the plateau. To verify this, we measured and plotted the response vs. 1/flow-rate curve under constant detector pressure. As Fig. 8 shows, the response is linear, which verifies that the PDHID is essentially a concentration-dependent detector.

### 3.4. Detector volume

As calculated in the Experimental section, the effective internal volume of the detector is 113 $\mu$l when the diameter of the ionization region is 3 mm. The volume of the ionization region decreases to 50 $\mu$l if the diameter is 2 mm and increases to 314 $\mu$l with a diameter of 5 mm. The effect of this internal volume on the response of the detector was evaluated using a 100 ppm $C_1$–$C_6$ hydrocarbon mixture in helium.

The response of the detector to the hydrocarbon mixture was evaluated as a function of helium flow-rate, in a manner similar to that discussed previously. Fig. 9 is a graph of the response to propane versus the reciprocal flow-rate for the various ionization chambers. The general shapes of the curves for all detector sizes are similar to those in Fig. 7. Obviously the

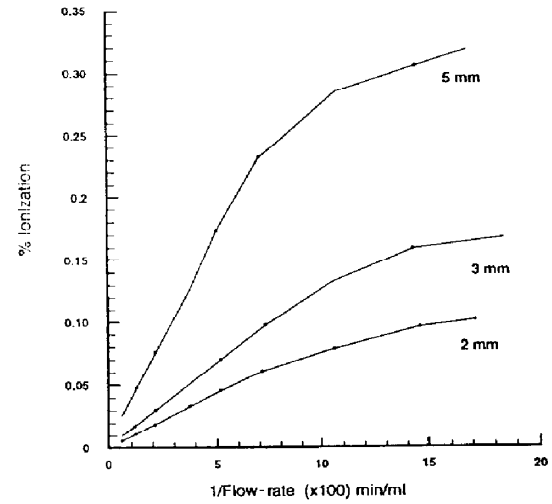


Fig. 9. Detector response (percent ionization) versus reciprocal flow-rate. Same conditions as Fig. 7 except different detector volumes, and only 6 $\mu$l sample size used (internal diameters are specified).

response for propane increases with increasing detector size. However, the increase in response is not directly proportional to the detector volume; in going from a 2 mm diameter to a 5 mm diameter the volume increases by a factor of ca. 6, whereas the response increases by a factor of ca. 4. But the standing current also increases with increasing detector volume, as shown in Fig. 10. An increased standing current increases the noise of the baseline, since a larger signal must be zeroed out by applying a larger bucking potential. This effectively negates any sensitivity gained from increased detector volume.

The factor of most concern to chromatographers is the effect of cell volume on the amount of flow required to yield a residence time which maintains the integrity of the chromatographic peak. Fig. 11 shows a chromatogram of the 100 ppm $C_1$–$C_6$ hydrocarbon mixture on the DB-5 column (30 m × 0.25 mm I.D., 1.0 $\mu$m film thickness). The chromatogram to the right in Fig. 11 was run with a faster chart speed to show the separation of the $C_1$–$C_3$ hydrocarbons. The methane and ethane are only just separated, but the $C_3$–$C_6$ hydrocarbons are well separated. However, note the water peak between $C_3$ and $C_4$ that tails into the $C_4$ peak. The water apparently comes from the sample loop, and could probably be reduced by heating.

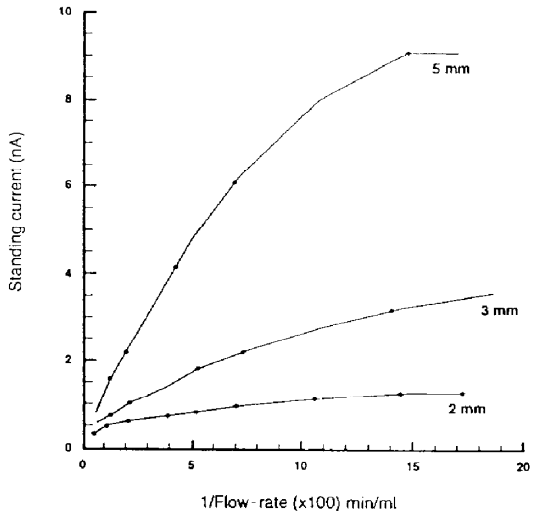


Fig. 10. Standing current versus reciprocal flow-rate. Same detector conditions as Fig. 7, except different detector volumes (internal diameters are specified).

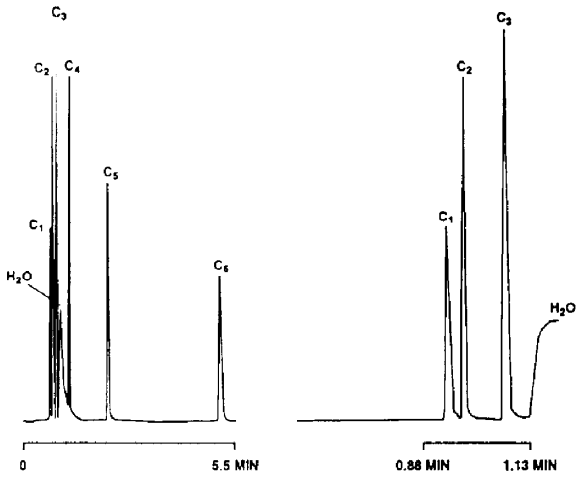


Fig. 11. Chromatograms of 100 ppm hydrocarbon mixture on the DB-5 column. Pulse interval: 300 $\mu$s; charging time of the coil: 40 $\mu$s; d.c. voltage to the coil: 20 V; bias voltage: 200 V; discharge flow-rate: 20 ml/min; sample size: 6 $\mu$l.

Because the $C_1$–$C_6$ hydrocarbon peaks have high resolution, this chromatogram gives a good test of detector performance. We measured both the peak area and the peak height for the $C_3$, $C_4$ and $C_5$ hydrocarbons, and determined the ratio of the area to the height as a function of the flow-rate through the detector. (The column flow-rate was kept constant, with only the helium flow through the discharge varied). This ratio should remain constant as long as the detector makes no contribution to peak broadening. A graph of the ratio versus reciprocal flow-rate shows a constant value at higher flow-rates, but a sharp increase at lower flow-rates, due to peak broadening from the increased detector residence time.

Fig. 12 shows the flow-rate at which each detector began to experience peak broadening for propane. As expected, the smallest volume detector (2 mm diameter/ca. 50 $\mu$l) could tolerate the lowest flow-rate, which was 11.4 ml/min ($8.7 \cdot 10^{-2}$ min/ml on the 1/flow-rate scale). This is probably the narrowest peak possible with this column. On the other hand, if the detector with the 5 mm diameter (ca. 314 $\mu$l) is used, the flow-rate must be 67 ml/min. For the 3 mm

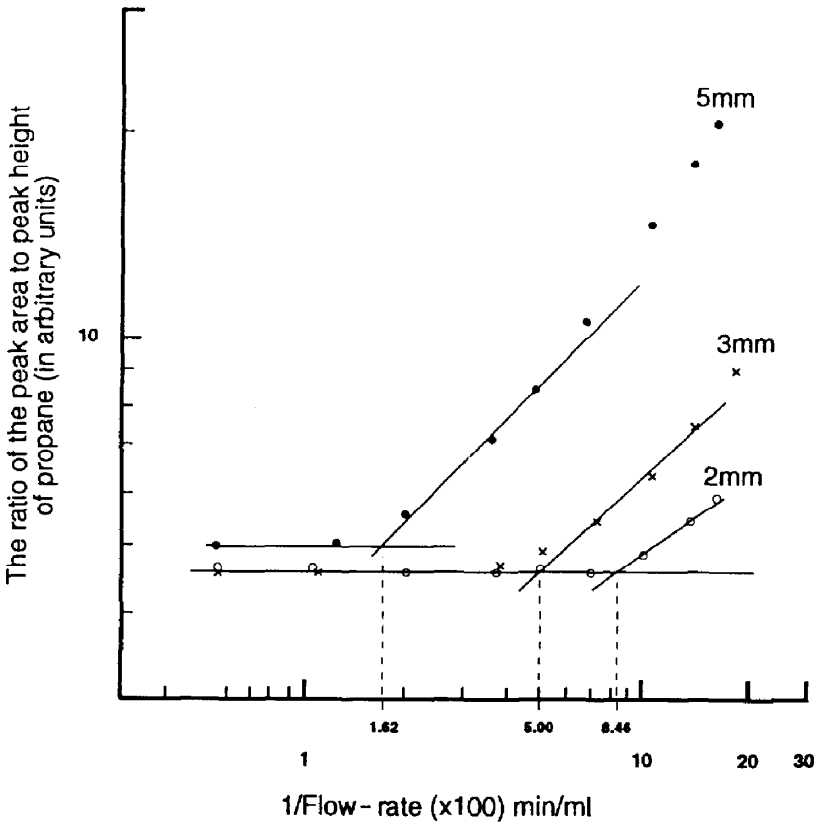


Fig. 12. Ratio of peak area to peak height of propane versus reciprocal flow-rate with different detector I.D. Pulse interval: 300 $\mu$s; charging time of the coil: 40 $\mu$s; d.c. voltage to the coil: 20 V; bias voltage: 200 V; discharge flow-rate: 20 ml/min.

detector (ca. 113 $\mu$l), a flow-rate of approximately 20 ml/min is required to prevent peak broadening for $C_3$. These requirements are consistent with a residence time of approximately 0.3 s, which seems adequate to resolve the $C_3$ peak with a base width of 1.4 s. Note that for the most part the required flow-rates fall on the linear portion of the curve, where the detector sensitivity is concentration-dependent. The required flow-rates and corresponding residence times for the $C_3$, $C_4$ and $C_5$ compounds for the three different detector diameters are shown in Table 1. Apparently a flow-rate of approximately 10 ml/min is sufficient for the 3 mm diameter detector. The 5 mm diameter detector requires an excessive flow-rate, on the order of 50 ml/

Table 1
Relationship between detector size and minimum flow-rate required

| Diameter/volume of the ionization region | Minimum flow-rate (residence time) for | | |
|---|---|---|---|
| | $n$-$C_3H_8$ | $n$-$C_4H_{10}$ | $n$-$C_5H_{12}$ |
| 2 mm/50 $\mu$l | 11.8 ml/min (0.25 s) | 8.5 ml/min (0.35 s) | – |
| 3 mm/113 $\mu$l | 20 ml/min (0.34 s) | 13.6 ml/min (0.50 s) | 9.0 ml/min (0.75 s) |
| 5 mm/314 $\mu$l | 62 ml/min (0.30 s) | 35.6 ml/min (0.53 s) | 27.4 ml/min (0.69 s) |
| Peak width | 1.4 s | 1.8 s | 2.7 s |

min, to adequately define the sharp peaks from a 0.25 mm I.D. column. However, the larger volume detector could be used successfully with megabore capillaries and packed columns where the gas chromatographic peaks are inherently broader.

### 3.5. Mode of ionization

In order to confirm the mode of ionization, the relative responses of numerous gases to the PDHID were measured and compared to those from a helium ionization detector (HID) [10] and a helium photo-ionization detector (HPID) [11]. As expected, the relative responses to the HID and HPID are quite different, since the ionization by helium-excited species should be quite different from ionization using photons from the helium resonance transition (58.4 nm). The data are shown in Table 2, where the responses are relative to methane. In general there is better agreement in the relative responses for the HID and the PDHID. (More than between the HID and the HPID). The greatest discrepancies are for $H_2$, $CO_2$ and $SO_2$.

Table 2
Detector response relative to methane on a per mol basis

| Analyte | Type of detector | | |
|---|---|---|---|
| | HID | PDHID | HPID |
| $H_2$ | 0.35 | 0.19 | 2.01 |
| $N_2$ | 0.47 | 0.40 | 0.42 |
| Ar | 0.53 | 0.60 | 0.49 |
| $O_2$ | 0.65 | 0.59 | 0.36 |
| CO | 0.71 | 0.51 | 0.42 |
| $CH_4$ | 1.00 | 1.00 | 1.00 |
| $SF_6$ | 1.11 | 0.89 | 0.22 |
| $C_2H_6$ | 1.65 | 1.85 | 1.12 |
| $C_2H_4$ | 1.94 | 1.40 | 0.78 |
| $C_3H_8$ | 2.35 | 2.48 | 0.57 |
| $C_4H_{10}$ | 2.65 | 3.23 | – |
| $CO_2$ | 3.29 | 0.98 | 0.27 |
| $H_2S$ | 3.06 | 1.65 | – |
| $N_2O$ | 3.29 | 0.92 | 0.34 |
| $SO_2$ | 3.29 | 1.61 | 0.75 |

### 3.6. Emission spectra from $He_2$

The emission spectrum from the discharge in helium was recorded using the monochromator described previously. The only helium emission spectra is the broad band in the vicinity of 70–90 nm. This is the well-known Hopfield emission which arises from the transition

$$He_2(A\ ^1\Sigma_u^+) \rightarrow 2\ He(1\ ^1S) + h\nu$$

The reason for the broad emission is the dissociative ground state. It would seem that this photoemission plays the dominant role in the ionization mechanism.

Since the PDHID response depends upon the $He_2$ continuum, with energies in the range 16–18 eV, it is understandable why the PDHID responses in Table 2 differ from the HPID responses, which depend upon the He resonance line at 21.2 eV. Of particular note is the low response of the HPID for $C_3H_8$ compared to the PDHID response. This might suggest that the HPID response to longer-chain hydrocarbons may be low, whereas with the PDHID, as we will see shortly, the molar response of the hydrocarbons increases with chain length.

The lower energy range of the vacuum UV emission spectra from the discharge consists of atomic emissions from other elements in the discharge. The background generally consists of atomic emission from N, O and H, which probably arise from air and water. The emission spectra from the pulsed discharge source can be used for specific element identification. The most useful emission spectra for the lighter atoms fall in the vacuum UV region from 100–200 nm. This is being investigated extensively and at the present time it appears to be effective for the detection of Cl, Br, I and S.

### 3.7. Percent ionization

The percent ionization for the PDHID has been determined for certain selected gases, with the results shown in Table 3. Generally the percent ionization increases with molecular size,

Table 3
Relative responses for various classes based on propane

| Analyte | Molecular mass | Percent ionization | Relative response (to $C_3$) | |
|---|---|---|---|---|
| | | | per mol | per gram |
| *n-Alkanes* | | | | |
| Methane | 16.0 | 0.0099 | 0.404 | 1.11 |
| Ethane | 30.1 | 0.0184 | 0.751 | 1.10 |
| Propane | 44.1 | 0.0245 | 1.00 | 1.00 |
| *n*-Butane | 58.1 | 0.0320 | 1.31 | 0.99 |
| *n*-Pentane | 72.2 | 0.0423 | 1.73 | 1.06 |
| *n*-Hexane | 86.2 | 0.0503 | 2.05 | 1.05 |
| *n*-Heptane | 100.2 | 0.0579 | 2.36 | 1.04 |
| *n*-Octane | 114.2 | 0.0660 | 2.69 | 1.04 |
| *n*-Nonane | 128.3 | 0.0761 | 3.11 | 1.07 |
| *Branched alkanes* | | | | |
| 2-Methylpropane | 58.1 | 0.0341 | 1.39 | 1.06 |
| 2,2-Dimethylbutane | 86.2 | 0.0555 | 2.27 | 1.16 |
| 3,3-Dimethylpentane | 100.2 | 0.0592 | 2.42 | 1.06 |
| 3-Ethy pentane | 100.2 | 0.0561 | 2.29 | 1.01 |
| 2,2,4,4-Tetramethylpentane | 128.3 | 0.0711 | 2.90 | 1.00 |
| *Unsaturated and ring hydrocarbons* | | | | |
| Ethylene | 28.1 | 0.0128 | 0.522 | 0.82 |
| 1-Propene | 42.1 | 0.0217 | 0.885 | 0.93 |
| 1-Butene | 56.1 | 0.0287 | 1.17 | 0.92 |
| 1-Pentene | 70.2 | 0.0353 | 1.44 | 0.90 |
| 1-Hexane | 84.1 | 0.0463 | 1.89 | 0.99 |
| 1,3-Butadiene | 54.1 | 0.0270 | 1.10 | 0.90 |
| Cyclohexane | 84.2 | 0.048 | 1.96 | 1.03 |
| Cyclohexene | 82.1 | 0.038 | 1.55 | 0.83 |
| *Permanent gases* | | | | |
| Nitrogen | 28.0 | 0.00400 | 0.163 | 0.26 |
| Hydrogen | 2.02 | 0.00187 | 0.076 | 1.67 |
| Oxygen | 32.0 | 0.00594 | 0.242 | 0.33 |
| Argon | 39.9 | 0.00594 | 0.242 | 0.27 |
| Carbon monoxide | 28.0 | 0.00510 | 0.208 | 0.33 |
| Carbon dioxide | 44.0 | 0.00980 | 0.400 | 0.40 |
| Sulfur dioxide | 64.1 | 0.01610 | 0.657 | 0.45 |
| Sulfur hexafluoride | 146.1 | 0.00883 | 0.360 | 0.11 |
| *n-Alcohols* | | | | |
| Methanol | 32.0 | 0.0134 | 0.547 | 0.75 |
| Ethanol | 46.1 | 0.0222 | 0.906 | 0.87 |
| *n*-Propanol | 60.1 | 0.0312 | 1.27 | 0.93 |
| *n*-Butanol | 74.1 | 0.0375 | 1.53 | 0.91 |
| *n* Pentanol | 88.2 | 0.0404 | 1.65 | 0.83 |
| *sec.-Alcohols* | | | | |
| 2-Propanol | 60.1 | 0.0308 | 1.26 | 0.92 |
| 2-Butanol | 74.1 | 0.0397 | 1.62 | 0.96 |

*(Continued on p. 146)*

Table 3 (*continued*)

| Analyte | Molecular mass | Percent ionization | Relative response (to $C_3$) | |
|---|---|---|---|---|
| | | | per mol | per gram |
| *Aromatics* | | | | |
| Benzene | 78.1 | 0.037 | 1.51 | 0.85 |
| Toluene | 92.1 | 0.044 | 1.80 | 0.86 |
| Ethylbenzene | 106.2 | 0.049 | 2.00 | 0.83 |
| *n*-Propylbenzene | 120.2 | 0.055 | 2.24 | 0.82 |
| *Chlorine compounds* | | | | |
| Dichloromethane | 84.9 | 0.0286 | 1.17 | 0.61 |
| Trichloromethane | 119.4 | 0.0422 | 1.72 | 0.63 |
| Tetrachloromethane | 153.8 | 0.0535 | 2.18 | 0.62 |
| *Bromine compounds* | | | | |
| Dibromomethane | 173.8 | 0.0353 | 1.44 | 0.36 |
| Tribromomethane | 252.7 | 0.0387 | 1.58 | 0.28 |

ranging from 0.002% for $H_2$ to 0.08% for nonane. Note that the $C_4$ compounds with different amounts of unsaturation and structure all have similar percent ionizations of 0.030–0.034%, whereas the one $C_3$ compound has a lower percent ionization of 0.025%.

Percent ionization is dependent on the parameters discussed previously: pulse discharge interval, pulse discharge power and helium flow-rate through the discharge region. The values used to obtain the data in Table 3 are somewhat typical: 300 $\mu$s interval between pulses, charging time of 40 $\mu$s at 20 V, and helium flow-rate of 40 ml/min. With the exception of a few permanent gases, the percent ionization falls in the range 0.01–0.08% for compounds of $C_9$ or less. This range of percent ionization can be compared to the typical percent ionization for other types of ionization detectors: 0.0005% for an FID, 0.3% for a helium photoionization detector [11] (which uses a microwave-induced discharge source and operates at low pressure), and 5% for a radioactive helium ionization detector. (Table 4)

Even though there is a great range in percent ionization among the detectors in Table 4, the background noise also varies considerably, gen-

Table 4
Ionization efficiency and relative sensitivity of some ionization detectors

| | FID [10] | HPID [11] | HID [10] | PDHID (This work) |
|---|---|---|---|---|
| Apparent ionization efficiency (propane) | 0.000005 | 0.003 | 0.05 | 0.0007 |
| Noise level (A) | $1 \cdot 10^{-14}$ | $4 \cdot 10^{-11}$ | $2.5 \cdot 10^{-12}$ | $1.2 \cdot 10^{-13}$ |
| Percent ionization/noise | $5 \cdot 10^{8}$ | $7.5 \cdot 10^{7}$ | $2 \cdot 10^{10}$ | $5.8 \cdot 10^{9}$ |
| Relative sensitivity | 1.0 | 0.15 | 40 | 12 |
| Linear dynamic range | $10^{7}$ | $10^{4}$ | $10^{3}$ | $10^{5}$ |
| Carrier gas | Air/$H_2$ | He | He | He |
| Substances | Most organics | Universal | Universal | Universal |

erally increasing as percent ionization increases. Consequently, the sensitivity $\alpha$ (percent ionization/noise) varies by a factor of only 40 from FID to HID. The PDHID is more sensitive than the FID by a factor of ca. 12, but less sensitive than the HID by a factor of ca. 4. Note that the HID sensitivity is greatest; however, it is not a satisfactory detector for higher boiling organic compounds, since they would tend to absorb on the tritium foil. The PDHID sensitivity for propane is an order of magnitude greater than the FID and two orders of magnitude greater than the HPID. The linear dynamic range is greatest for the FID ($10^7$), but the range of $10^5$ for the PDHID should be satisfactory in most cases. Of more importance is the fact that the PDHID response is universal, whereas the FID is restricted to organics.

### *3.8. Relative response for various classes of compounds*

Table 3 shows the relative responses for several classes of compounds. As noted previously, the relative responses on a mole basis for the hydrocarbons increases with increasing carbon number. This is most apparent for the straight-chain hydrocarbons $C_1$–$C_9$, where the relative response changes from 0.50 to 3.11. Apparently the cross-section for ionization increases with increasing molecular size and the response increases in a manner similar to that for an FID. The last column of Table 3 shows the relative response on a per gram basis. Note that the responses for the *n*-$C_2$ to *n*-$C_9$ hydrocarbons vary by ca. 10%.

Also shown in Table 3 are the relative responses for branched hydrocarbons. On a per gram basis these values fall in the range 1.0–1.16. A few cyclic and unsaturated hydrocarbons, also given in Table 3, have relative responses ranging from 0.83 to 1.03. The relative responses for some aromatic hydrocarbons in Table 3 tend to be lower than those for saturated hydrocarbons, ranging from 0.82 to 0.86. The relative responses of the $C_1$–$C_5$ alcohols (Table 3) fall in the 0.75–0.93 range. Since these responses are below those for the saturated hydrocarbons, the OH is apparently less susceptible to ionization than a $CH_3$ group. With the exception of methane, the relative response per gram for all hydrocarbons and alcohols, regardless of structure, falls in the 0.75–1.16 range.

The relative responses of some chloro- and bromomethanes were also determined. The values for the chloro compounds are ca. 0.6 and for the bromo compounds ca. 0.3. One would expect the relative response for the halogenated compounds to be significantly less, because there are numerous electrons that are tightly held and probably not accessible for ionization. In the chloro compounds the 1s, 2s and 2p electrons are tightly held and probably do not contribute significantly to the ionization. Similarly, for the bromine atom the 1s, 2s, 2p, 3s and 3p electrons would not be ionized.

### *3.9. Concentration dependence*

Concentration dependence was determined using the response to propane mixtures in helium. The detector with a 3 mm diameter was used, with a flow-rate of 20 ml/min. Six gas mixtures were prepared that ranged from $4.95 \cdot 10^{-5}$ to $9.13 \cdot 10^{-3}$ parts by volume. Three different sample volumes were used: 0.06, 5.0 and 50.0 $\mu$l. The 0.06-$\mu$l sample came from the sampling valve in which the sample is measured by an internal engraving on the rotor. (The volume of 0.06 $\mu$l is approximate, and should be calibrated with a larger, more accurately measured sample loop. In this study we assumed the 50-$\mu$l loop to be accurate and calibrated the 0.06-$\mu$l and 5.0-$\mu$l loops against it).

Fig. 13 shows a typical log–log plot of the response for propane versus the mass injected, using sample volumes of 0.6, 5.0 and 50.0 $\mu$l. The responses for the 0.6- and 5.0-$\mu$l volumes were corrected according to the calibration described previously. The straight line shows a slope of one, representing a linear relationship between response and concentration. Note that the data fit the straight line quite well until the concentration reaches $1 \cdot 10^5$ pg, shown by the dashed vertical line. The linear range in Fig. 13 extends over four orders of magnitude. Since the

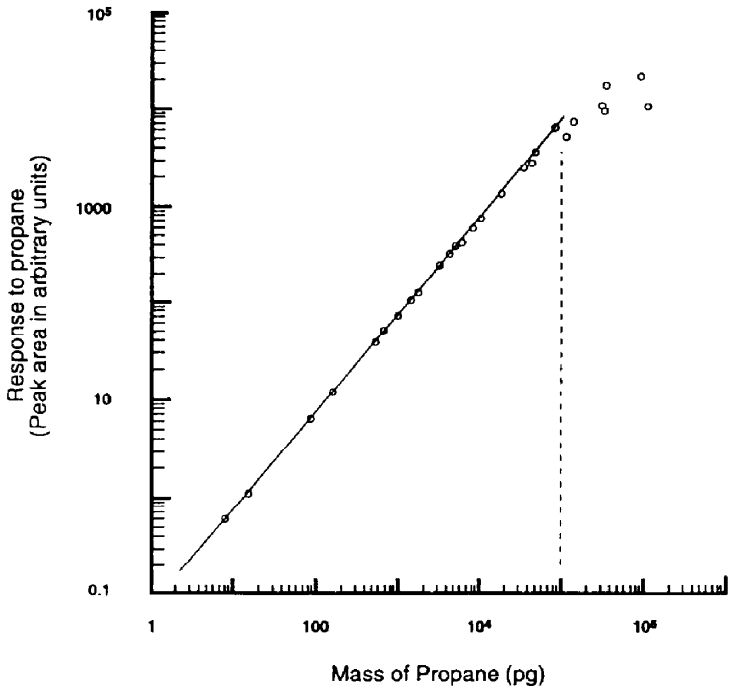


Fig. 13. Log relative response to propane versus mass of propane injected. Data using the 0.06-$\mu$l and 5.0-$\mu$l calibrated against the 50-$\mu$l loop. Same detector conditions as Fig. 11.

minimum detectable amount of propane is ca. 0.8 pg, the linear dependence could be extended by an additional order of magnitude. Consequently, the detector would be linear over a total range of five orders of magnitude.

The test of linearity is also shown in Fig. 14, where the percent ionization is graphed versus the logarithm of the injected mass of propane. In this type of graph a constant value of the percent ionization designates the linear concentration dependence of the detector. When the detector starts to become saturated there is a sharp decrease in percent ionization, as observed in Fig. 14 at approximately $10^5$ pg = 100 ng.

### 3.10. Analysis of permanent gases

For many years helium ionization detectors have been used in conjunction with a 5A molecular sieve GC column to detect the so-called permanent gases (Ne, $H_2$, Ar, $O_2$, $N_2$, $CH_4$ and CO). Because of its importance to research and production in the solid-state industry, this analysis deserves special attention in our study of the PDHID. Although we reported on this analysis in a previous publication [1], that study involved a different flow configuration that allowed the analytes to pass through the discharge region. Because the current detector does *not* allow this we might expect a change in sensitivity, particularly toward gases like the permanent gases in which the ionization potentials range from 12.06 eV for $O_2$ to 21.564 eV for Ne.

The previous study used a packed 5A molecular sieve column, 5 ft. × 1/8 in. O.D. (1 ft. = 30.48 cm, 1 in. = 2.54 cm). This study employs a 5A molecular sieve porous layer open tubular (PLOT) column, 30 mm × 0.32 mm I.D. (Chrompack, Raritan, NJ, USA). Fig. 15 shows chromatograms of the permanent gases on this column at 25°C, where Ar and $O_2$ have separate

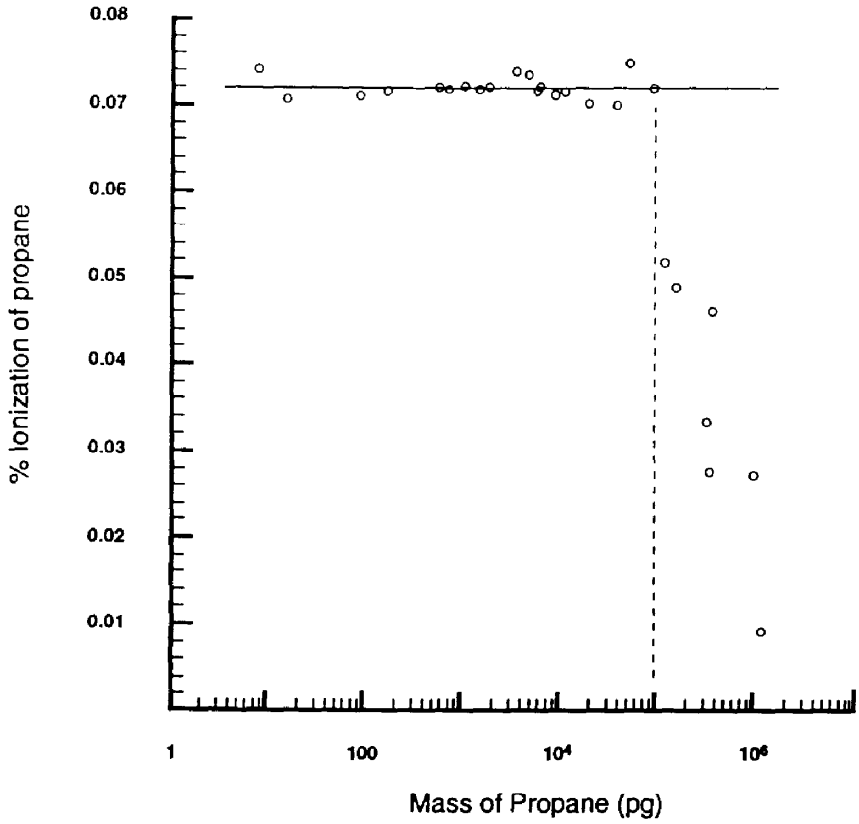


Fig. 14. Percent ionization versus log mass of propane. Same detector conditions as Fig. 13.

peaks, and at 100°C, where Ar and $O_2$ elute as one peak but the CO elutes in a reasonable length of time. The separation at 100°C is comparable to the results obtained in the previous study with the packed column at 95°C [1].

Because the Ar and $O_2$ were eluted simultaneously in the previous study we cannot compare the results with the current study in which a different $Ar/O_2$ concentration ratio was used. It is also risky to compare the sensitivity for $N_2$, since it is susceptible to possible air leakage into the sample. The sensitivities for the other permanent gases, expressed as minimum detectable quantity (MDQ), are given in Table 5, along with the values from the previous study [1]. In general it appears that the sensitivity of the PDHID used in this study is lower for these permanent gases by a factor of 5–10. Apparently the enhanced sensitivity realized in the first study arises from the direct ionization that occurs as the analytes pass through the pulsed discharge. As might be expected, the most dramatic difference between the sensitivities of the two configurations shows up with neon —its ionization potential of 21.564 eV makes it the most difficult of the permanent gases to ionize. The response from the PDHID used in this study is low because the energy of the $He_2$ emission responsible for analyte ionization (17.86–19.7 eV) is less than neon's ionization potential.

While this section demonstrates that greater sensitivity is realized when the analytes are allowed to pass through the discharge, this advantage is offset by the potential problems that may arise when a solvent or a large sample such as air disrupts the discharge.

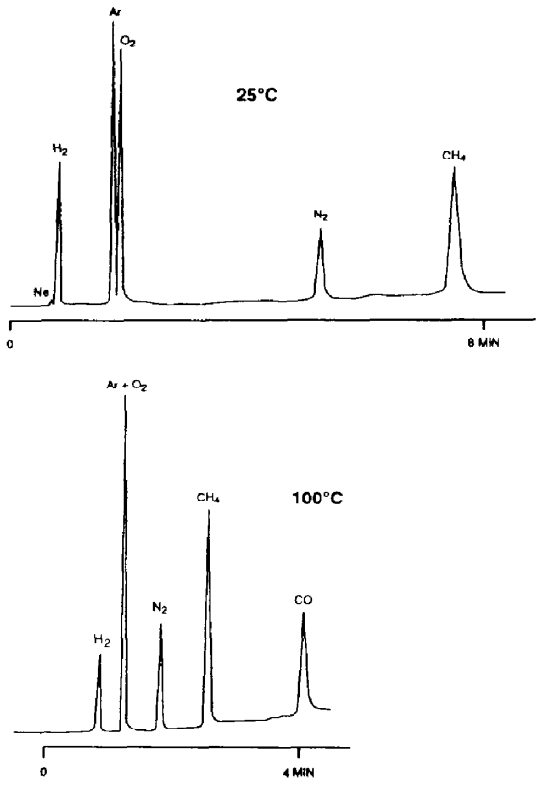


Fig. 15. Chromatograms of the permanent gases with column temperatures of 25 and 100°C. Column: Chrompack PLOT, fused-silica 5A molecular sieve, 25 m × 0.32 mm; detector: PDHID, flow-rate 20 ml/min, temperature 25°C; sample: 2 ppm, 50-$\mu$l sample loop.

### 3.11. Application to high-speed chromatography

As discussed previously, the analyte residence time in the PDHID is about 0.3 s with a 3 mm I.D. detector cell and 20 ml/min flow-rate. With a smaller I.D. detector cell and higher detector flow-rate the residence time is even briefer. This fast response feature makes it possible to apply the PDHID to high-speed chromatographic analysis. Fig. 16 illustrates one example of BTEX (benzene, toluene, ethylbenzene, xylenes) analysis with the PDHID and a microbore column (DB-1701, 10 m × 0.05 mm, 0.05 $\mu$m film thickness). The complete BTEX analysis in this example takes only 2.5 min, compared to ca. 20 min typical for normal GC analysis.

The sharp, symmetric BTEX peaks indicate that the PDHID gives a fast response to these components, but the technique has some limitations. A large sample loop cannot be used because the sample will be broadened under such a slow column flow-rate (0.1 ml/min). Consequently, the overall sensitivity of this method is not as high as normal GC analysis —a small amount of highly concentrated sample must be used to get significant response. This experiment used a valve with an 0.06-$\mu$l internal loop as an injector. Some other injection techniques, such as the cryogen concentration meth-

Table 5
Minimum detectable quantity (MDQ) of permanent gases

| | MDQ (pg) | | |
|---|---|---|---|
| | Column 25°C [a] | Column 100°C [a] | Column 95°C [b] |
| Neon | 39.8 | 42.4 | 1.4 |
| Hydrogen | 0.23 | 0.31 | 0.04 |
| Argon | 1.68 | 2.48 | 0.8 |
| Oxygen | 2.46 | | |
| Nitrogen | 3.28 | 1.58 | 1.9 |
| Methane | 2.47 | 1.02 | 0.1 |
| Carbon monoxide | – | 3.25 | 0.7 |

[a] This study.
[b] From Ref. [1].

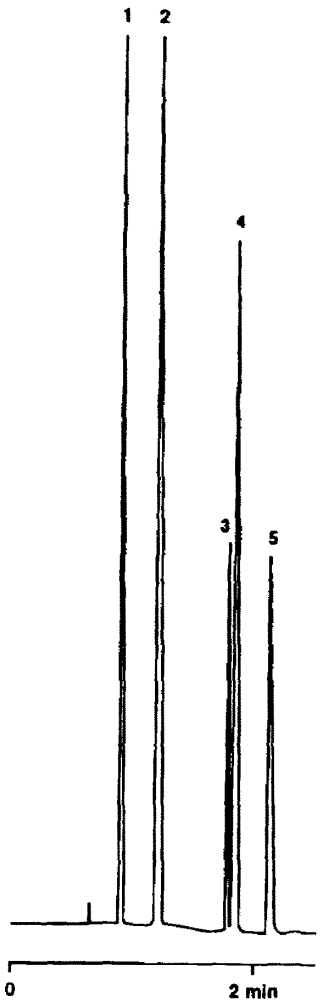


Fig. 16. Chromatogram of aromatics obtained by using PDHID and microbore columns. Column: J&W DB-1701, 10 m × 0.05 mm, film thickness 0.05 μm; detector: PDHID, flow-rate 20 ml/min; injector: split, 1:150 ratio. Peaks: 1 = benzene; 2 = toluene; 3 = ethylbenzene; 4 = *m,p*-xylene; 5 = *o*-xylene.

od, could help to increase the sensitivity of the high-speed gas chromatograph.

### *3.12. High-temperature operation*

The results discussed before were obtained from a PDHID with Vespel as the insulation material. At high detector temperature, this detector has two major problems. First, the Vespel decomposes and produces compounds which enter the detector cell, resulting in reduced response. Consequently, the response of the detector continually decreases as the temperature increases. The response at 200°C is only half the response at 30°C. The other problem is electrical conductivity. The experiments show that the electrical leakage through the Vespel makes a measureable contribution to the standing current at about 150°C, and increases exponentially with increasing temperature. The maximum detector temperature at which the electrical leakage can be tolerated is about 200°C, which is not high enough for some applications.

At present, we are considering insulating materials that will allow the PDHID to operate at temperatures on the order of 350°C. Quartz, sapphire and high-density alumina have been shown to be satisfactory. The metal electrode poses an additional material consideration: at 350°C, there is a potential for it to act as a heterogeneous catalyst. The results of these studies will be reported in a future publication.

## Acknowledgements

The authors would like to thank Larry Sims from the Electronics Shop (University of Houston) for his assistance in the design and repair of electronic components. We would also like to thank David Salge, technical writer at Valco Instruments, for his assistance in preparing the text and illustrations for this manuscript. This research was supported by a grant from Valco Instruments Co. Inc., Texas ATP grant 003652-108, and the Robert A. Welch Foundation, grant E-095.

## References

[1] W.E. Wentworth, S.V. Vasnin, S.D. Stearns and C.J. Meyer, *Chromatographia*, 34 (1992) 219.
[2] W.E. Wentworth, E.D. D'Sa, H. Cai and S.D. Stearns, *J. Chromatogr. Sci.*, 30 (1992) 478.

[3] B.D. Quimby and J.J. Sullivan, *Anal. Chem.*, 62 (1990) 1027.
[4] R.B. Costanzo and E.F. Barry, *Anal. Chem.*, 60 (1988) 826.
[5] B.M. Patel, E. Heithmar and J.D. Winefordner, *Anal. Chem.*, 59 (1987) 2374.
[6] R.J. Skelton, P.B. Farnsworth, K.E. Markides and M.L. Lee, *Anal. Chem.*, 61 (1989) 1815.
[7] G.W. Rice, A.P. D'Silva and V.A. Fassel, *Appl. Spectros.*, 40B (1985) 1573.
[8] D.A. Ryan, S.M. Argentine and G.W. Rice, *Anal. Chem.*, 62 (1990) 1829.
[9] P.C. Uden (Editor), *Element-Specific Chromatographic Detection by Atomic Emission Spectroscopy*, American Chemical Society, Washington, DC, 1992.
[10] D.J. David, *Gas Chromatographic Detectors*, Wiley, New York, 1974.
[11] R.R. Freeman and W.E. Wentworth, *Anal. Chem.*, 43 (1971) 1987.
[12] S.V. Vasnin, W.E. Wentworth, S.D. Stearns and C.J. Meyer, *Chromatographia*, 34 (1992) 226.